Available online at www.sciencedirect.com
ScienceDirect
Thin Solid Films 516 (2008) 4018–4024
www.elsevier.com/locate/tsf

Fabry–Pérot fringes of hydrogen-bonded assembly films

Shuguang Yang, Shuaixia Tan, Yongjun Zhang, Jian Xu *, Xiaoli Zhang

State Key Laboratory of Polymer Physics and Chemistry, Joint Laboratory of Polymer Science and Materials, Institute of Chemistry, Chinese Academy of Sciences, Beijing 100080, China

Received 11 May 2006; received in revised form 16 July 2007; accepted 2 August 2007
Available online 14 August 2007

Abstract

Thin films were fabricated from poly(vinylpyrrolidone) (PVPON) and poly(acrylic acid) (PAA) based on hydrogen bonding layer-by-layer (LBL) assembly process. Due to light interference, PVPON/PAA films present Fabry–Pérot fringes in the UV–Vis–NIR spectrum. LBL assembly constructed the film on both sides of substrate (double-side film), which are different to traditional vacuum deposition that forms the film only on one side of substrate (single-side film). The light interference processes of the double-and single-side films were fully analyzed. Using the peak positions and amplitude of the Fabry–Pérot fringes, the refractive index and thickness of the film can be evaluated. Furthermore, Fabry–Pérot fringes can be utilized to monitor the film's growth and water content variation in the film.
© 2007 Elsevier B.V. All rights reserved.

Keywords: Layer-by-layer assembly; Hydrogen bond; Fabry–Pérot fringes; Film interference

1. Introduction

For a long time, researchers have been seeking various methods, such as vacuum thermo deposition, chemical vapor deposition (CVD), molecular beam epitaxy (MBE), sol–gel process, electroless deposition, and spin coating, to fabricate thin films to meet the increasing demands in science and technology. In recent years, a method named layer-by-layer (LBL) assembly has been developing to fabricate composite films with tailored structure. Decher et al. definitely described LBL assembly by alternately depositing positively and negatively charged polymers on a charged surface in the early 1990s [1,2]. This electrostatic assembly process allows for incorporation of a wealth of materials, such as proteins, DNA, virus, inorganic nanoparticles, and exfoliated clay sheets, into the construction of the thin films [3–5]. However, the other molecular interactions such as hydrogen bond [6,7], charge-transfer interaction [8,9], coordination bond [10,11], and even covalent bonds [12,13], can also provide choice to drive the LBL assembly process. In particular, hydrogen bonding assembly is deserved to pay attention to. Hydrogen bonds, as a kind of readily reversible molecular interactions, can induce supramolecular ordering and plays the essential roles in the key steps in the dance of life, e.g. DNA replication, protein folding, the specific enzyme recognition and the detection of molecular signals. Furthermore hydrogen bonding is generally sensitive to pH and ion strength, which are very useful to the controlled release and encapsulation [14].

Film interference is a common light phenomenon. When the film's thickness reaches to the level of a quarter of wavelength of the visible light, generally we can observe the light interference with naked eyes. However, to classic electrostatic LBL system, such as PAH/PSS, the film only increases with about 1 nm per assembly cycle [15], therefore the fabrication of a several-hundred-nanometer-thick film is a very arduous work. Improving the ion strength of the assembly solutions, the increment of per assembly cycle can largely increase, but higher ion strength enhances the roughness of the film [16], which would scatter light away and disturb the film interference. Stockton and Rubner reported hydrogen-bonded LBL assembly of polyaniline (PANi) with a number of different nonionic, water-soluble polymers including poly(vinylpyrrolidone) (PVPON), poly(vinyl alcohol) (PVA), poly(acrylamide) (PAAm), and poly(ethylene oxide) (PEO) [6]. At the same time they compared the hydrogen bonding assembly films with the electrostatic assembly film (PANi/PSS), and found that hydrogen bonding assembly tends to produce the more

---

* Corresponding author.
E-mail address: jxu@iccas.ac.cn (J. Xu).

0040-6090/$ - see front matter © 2007 Elsevier B.V. All rights reserved.
doi:10.1016/j.tsf.2007.08.010

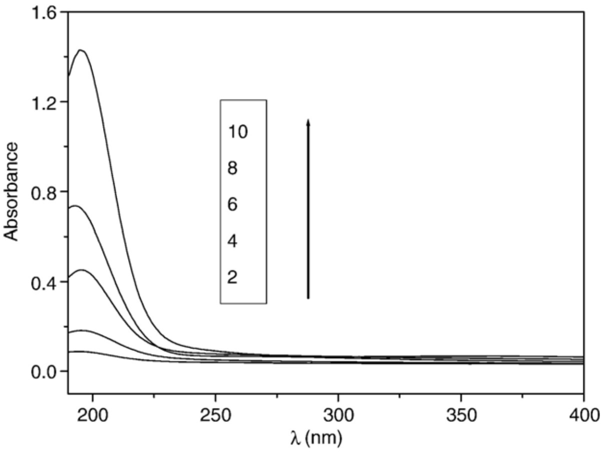

Fig. 1. UV spectra of (PVPON/PAA)$_n$ films for values of n varying from 2 to 10 cycles.

interpenetrated structure and thicker film because the charged repulsion among the polymer segments was almost avoided. Recently, we found that LBL assembling PVPON and PAA based on hydrogen bonding can produce the thicker and smoother film compared to its electrostatic counterparts, and the film often exhibited many oscillations (Fabry–Pérot fringes) in the UV–Vis–NIR spectrum. In this paper, we will fully analyze this light interference process of the LBL film, and elaborately demonstrate how to use the information derived from Fabry–Pérot fringes to determine the film's thickness and refractive index. At the same time, Fabry–Pérot fringe will be introduced as a simple but effective way to monitor the film's growth and composition variation.

2. Experiment

2.1. Materials

PAA sodium salt (Mw = 8000) and lithium fluoride (LiF) were purchased from Aldrich. PVPON (K30, Mw = 40,000), hydrochloric acid (HCl, 36.5%) and sodium hydroxide were received from Beijing Chemical Reagent Co.

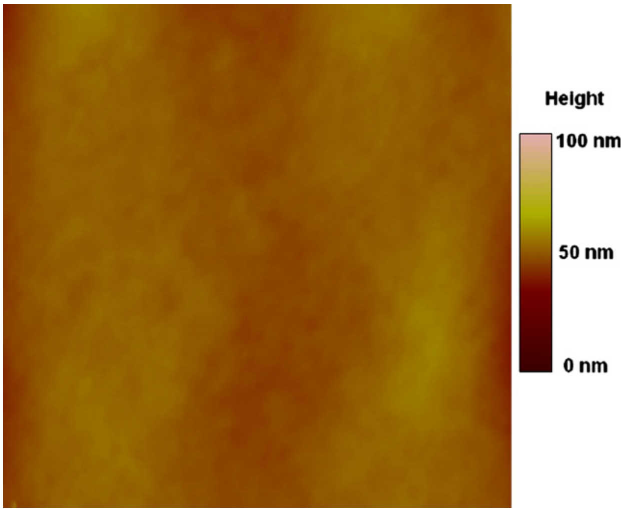

Fig. 2. AFM image (10 μm × 10 μm) of the (PVPON/PAA)$_{16}$ film.

2.2. Preparation of the films

2.2.1. LBL films (double-side films)

The hydrogen-bonded PVPON/PAA films were fabricated on quartz or glass substrates. Before assembling, the substrates were thoroughly cleaned: first immersed in a boiling H_2SO_4/H_2O_2 mixture (7:3 (v/v)) for 30 min, then rinsed with deionized water thoroughly, and finally dried with a stream of pure N_2. The pH values of the 1% (w/w) PVPON and PAA aqueous solutions and of the rinsing solutions were adjusted to 2 and 2.5, respectively, using HCl and NaOH solution. The films were fabricated with an automated machine (North Tianfu Ltd., Beijing, China) at the temperature of 25 ± 2 °C. The substrates were alternately immersed in the PVPON and PAA solutions for 4 min, with three rinsing intervals, 1 min each, to remove the excess of polymers. The number of assembly cycles was varied from 10 to 20. The sample name (PVPON/PAA)$_n$ designates film was made PVPON and PAA using n assembly cycle(s).

The LBL assembly constructed the PVPON/PAA film on both sides of the substrate. PVPON/PAA film is hydrogen-bonded and it can be disintegrated at higher pH values [14]. The PVPON/PAA film at one side of the substrate was removed with 0.1 M NaOH solution to get the single-side film.

2.2.2. Vacuum evaporation of LiF film (single-side film)

The LiF film was formed on a quartz substrate by vacuum deposition under a pressure of 3×10^{-4} Pa. The thickness of the thin film was monitored by a quartz crystal oscillator placed near the substrate and was calibrated *ex situ* by an Ambios Technology XP-2 surface profilometer, and the film thickness is about 270 nm.

2.3. Characterization

The UV–Vis–NIR spectra were recorded on a Shimadzu UV-1601 PC spectrophotometer (Spectroscopic range: from

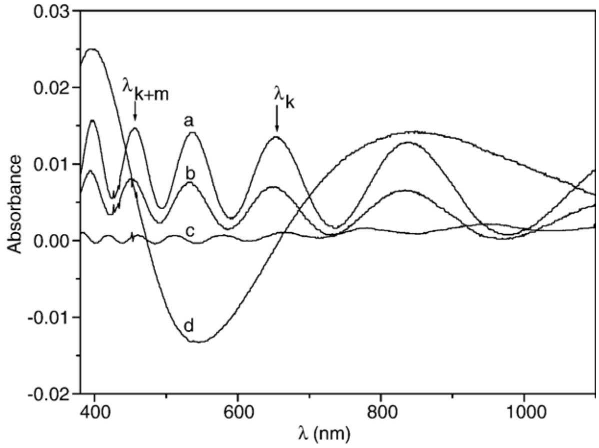

Fig. 3. Vis–NIR spectra: (a) double-side and (b) single-side (PVPON/PAA)$_{16}$ film on a quartz slide; (c) single-side (PVPON/PAA)$_{16}$ film on a glass side; (d) Lif film on a quartz slide. In the spectrum (a), λ_k and λ_{k+m} are the kth and $(k+m)$ th level interference peaks respectively (in this example m = 2).

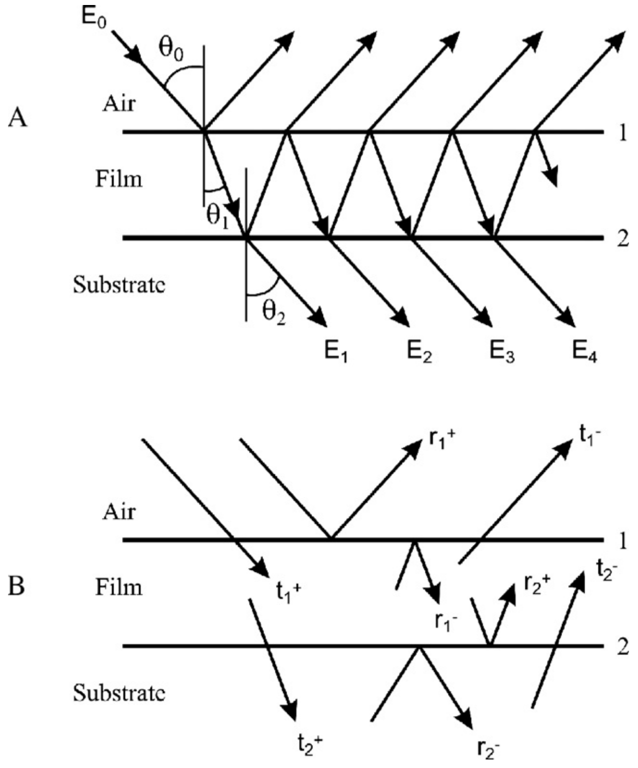

Scheme 1. (A) a light beam propagates via air-film and film-substrate interface, (B) illustration of the direction of the transmitted and reflected lights via the interfaces.

190 to 1100 nm). Atomic force microscopy (AFM) measurements were carried out in air at room temperature on a Nanoscope IIIA machine (Digital Instruments, Inc., USA) under the tapping mode. Commercial silicon probes (model TESP-100) with a typical resonant frequency of approximately 300 kHz were used to obtain the images. IR spectra were measured on a Bruke Equinox 55 spectrophotometer.

3. Results and discussion

3.1. Fabry–Pérot fringes of the PVPON/PAA film

PVPON and PAA can form the hydrogen-bonding interpolymer complex in aqueous solution [17], and recently we fabricated the composite film containing poly(methylsilsesquioxane) (PSQ) via LBL process based on hydrogen bonding between PVPON and PAA [18]. As long as the pH values of the assembling and rinsing solution were rigidly controlled ($pH<4$), the PVPON and PAA can been easily assembled on the substrate to construct the films.

UV–Vis spectrometer was applied to monitor the assembly process of PVPON and PAA. As shown in Fig. 1, the absorbance of the film is quickly increasing as the assembly process going on.

Mi et al studied the miscibility of the PVPON/PAA complex using ^{13}C solid state NMR, and estimated that the homogeneity is down to the scale of ~15 Å [19]. The LBL assembled PVPON/PAA film can be looked as a kind of interpolymer complex too, but at the solid–liquid interface not in the solution. Therefore the PVPON/PAA film should be endowed the capacity to obtain a certain high homogeneity too. AFM was applied to scan the morphology of the PVPON/PAA film. As shown in Fig. 2, the AFM image shows that film is very smooth, and the root mean square (RMS) roughness is only 2.738 nm at the area of 10 μm × 10 μm.

The smooth surface avoids diffuse reflection and is in favor of the optical characterization. When a (PVPON/PAA)$_{16}$ film was characterized by the spectrometer, there were many oscillations in the spectrum, as shown in Fig. 3. These oscillations are named as Fabry–Pérot fringes which are stemmed from light interference caused by the film at the different wavelength values.

3.2. Analysis interference process of hydrogen-bonded film

As shown in Scheme 1, due to transmission and reflection at the interfaces of film-air and film-substrate, when a light beam from air, through the film and then into the substrate, will be split into many sub-beams, which are expressed as below:

$$\begin{aligned} &E_1 = t_1^+ t_2^+ E_0 \\ &E_2 = t_1^+ r_2^+ r_1^- t_2^+ e^{-j2\varphi} E_0 \\ &E_3 = t_1^+ r_2^+ r_1^- r_2^+ r_1^- t_2^+ e^{-j4\varphi} E_0 \\ &\cdots \end{aligned} \tag{1}$$

So the complex expression of the amplitude of the beams through the film propagated in the substrate, is given by

$$E_t = \sum_{i=1}^{\infty} E_i = \frac{t_1^+ t_2^+}{1 - r_2^+ r_1^- e^{-j2\varphi}} E_0 \tag{2}$$

E_0 is the amplitude of the incident beam and E_i is the amplitude of the ith emerging beam. t_1^+ and r_1^+ (t_2^+ and r_2^+) are the transmission and reflection coefficients for the air-film (film-substrate) interface, while t_1^- and r_1^-(t_2^- and r_2^-) are the transmission and reflection coefficients for the film-air (substrate-film) interface. 2φ is the difference of phase between two consecutive rays, which is determined by the difference of optical path δ.

$$2\varphi = \frac{2\pi}{\lambda} \times \delta \tag{3}$$

$$\delta = 2n_1 d\cos\alpha \tag{4}$$

In Eq. (4), d and n_1 is the thickness and refractive index of the film respectively, and α is the incident angle of the beams. In our case α is equal to zero therefore the differences of phase is expressed as:

$$2\varphi = \frac{2\pi}{\lambda} \times 2n_1 d, \tag{5}$$

then

$$\varphi = \frac{2\pi n_1 d}{\lambda} \tag{6}$$

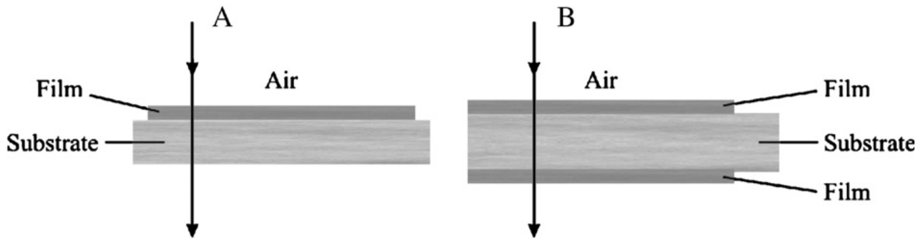

Scheme 2. Light transmits through the single-and double-side film respectively.

When the film and substrate are both dielectric and incident angle is zero, the transmission and reflection coefficients is expressed as below [20]:

$$r_1^+ = \frac{n_0 - n_1}{n_0 + n_1} = -r_1^- \tag{7}$$

$$r_2^+ = \frac{n_1 - n_2}{n_1 + n_2} = -r_2^- \tag{8}$$

$$t_1^+ t_1^- = \frac{4n_0 n_1}{(n_0 + n_1)^2} \tag{9}$$

$$t_2^+ t_2^- = \frac{4n_1 n_2}{(n_1 + n_2)^2} \tag{10}$$

n_0 and n_2 are refractive indexes of air and the substrate, respectively.

According to Eqs. (7) and (8), Eq. (2) was modified as

$$E_t = \sum_{i=1}^{\infty} E_i = \frac{t_1^+ t_2^+}{1 - r_2^+ r_1^- e^{-j2\varphi}} E_0 = \frac{t_1^+ t_2^+}{1 + r_1^+ r_2^+ e^{-j2\varphi}} E_0 = \frac{TE_0}{1 + \mathrm{Re}^{-j2\varphi}} \left(T = t_1^+ t_2^+, R = r_1^+ r_2^+\right) \tag{11}$$

When the light beams through the substrate enter into air again, there are two kind situations, Situation A (directly enter into air, single-side film) and Situation B (into air via a film, double-side film), as shown in Scheme 2. The vacuum deposition method can only construct film on the one side of the substrate, i.e. so-called the single-side film, which is corresponding to Situation A; however the LBL assembly can build the equivalent film on both sides of the substrate, i.e. so-called double-side film which is corresponding to Situation B.

There are three prerequisites to light interference: (1) equal frequency, (2) same direction, and 3) constant difference of phase. Atom irradiance is incontinuous. Different beams irradiated from an atom do not have the fixed phase-relationship therefore they can not interfere. In practical cases, only do the beams, which are split by one beam, have constant difference of phase. Moreover, a light beam has a limited life time therefore there exists a maximal interference length. When the difference of optical path exceeds the maximal interference length, there is no interference phenomenon. The maximal interference length (L_m) is estimated by

$$L_m = \frac{\lambda^2}{\Delta\lambda} \tag{12}$$

λ and $\Delta\lambda$ are the wave length and width of light source respectively.

To our UV–visible spectrometer, the scan scope is from 190 nm to 1100 nm, and spectroscopic width is 2 nm. So

$$Lm < \frac{(1100nm)^2}{2nm} = 605000nm = 0.605mm \tag{13}$$

However, the thickness of the substrate (quartz) is 1.2 mm and its refractive index is 1.46 at 550 nm. The difference of optical path contributed from the substrate is calculated as below

$$2n_2 d = 2 \times 1.46 \times 1.2mm = 3.504mm \tag{14}$$

Comparing Eq. (13) with Eq. (14)

$$Lm \ll 2n_2 d \tag{15}$$

That is to say, the substrate can not make light interference because it is too thick.

So the resulting amplitude of Situation A is the product of E_t (Eq. (11)) and the transmission coefficient of the substrate–air interface (t_A), and it is expressed as

$$E_{tA} = E_t t_A = \frac{t_A T}{1 + \mathrm{Re}^{-j2\varphi}} E_0 = \frac{T_A}{1 + \mathrm{Re}^{-j2\varphi}} E_0 \quad \left(T_A = t_A t_1^+ t_2^+\right) \tag{16}$$

Situation B is more complicated than Situation A. However, in Situation B, the amplitude can also be looked as a product of E_t and a complex transmission coefficient (t_B). LBL assembly on planar quartz forms a symmetry structure, i.e. the film on one side is equivalent to that on the other side. So the amplitude of LBL film (Situation B) is:

$$\begin{aligned} E_{tB} &= E_t t_B = \frac{t_1^+ t_2^+}{1 - r_2^+ r_1^- e^{-j2\varphi}} E_0 t_B \\ &= \frac{t_1^+ t_2^+}{1 - r_2^+ r_1^- e^{-j2\varphi}} E_0 \frac{t_2^- t_1^-}{1 - r_1^- r_2^+ e^{-j2\varphi}} = \frac{t_1^+ t_1^- t_2^+ t_2^-}{(1 + r_1^+ r_2^+ e^{-j2\varphi})^2} E_0 \\ &= \frac{T_B}{(1 + \mathrm{Re}^{-j2\varphi})^2} E_0 \left(T_B = t_1^+ t_1^- t_2^+ t_2^-\right) \end{aligned} \tag{17}$$

Accordingly, the transmitted intensity of Situation A and B, are respectively described as

$$I_{tA} \propto E_{tA} E_{tA}^* = \frac{(T_A)^2 E_0^2}{(1 + R)^2 - 4R\sin^2\varphi} \tag{18}$$

$$I_{tB} \propto E_{tB} E_{tB}^* = \frac{(T_B)^2 E_0^2}{((1 + R)^2 - 4R\sin^2\varphi)^2} \tag{19}$$

Subsequently the absorbance of the films, ABS, are expressed as

$$\mathrm{ABS}_A = -\log\frac{I_{tA}}{I_0} = \log\frac{(1+R)^2 - 4R\sin^2\varphi}{(T_A)^2} \tag{20}$$

$$\mathrm{ABS}_B = -\log\frac{I_{tB}}{I_0} = \log\frac{[(1+R)^2 - 4R\sin^2\varphi]^2}{(T_B)^2} \tag{21}$$

From Eqs. (7), (8) and (11), the expression of R is given by

$$R = r_1^+ r_2^+ = \frac{n_0 - n_1}{n_0 + n_1}\frac{n_1 - n_2}{n_1 + n_2} \tag{22}$$

(i) In case of $n_0 = n_1$ or $n_1 = n_2 \rightarrow R = 0$

That is to say, if the refractive index of the medium is equal to that of the film or the refractive index of the film is equal to that of the substrate, there will be no Fabry–Pérot fringes present in the spectrum.

(ii) In case of $n_0 < n_1 < n_2 \rightarrow R > 0$

When $\sin^2\varphi = 0$, the absorbance has maximal values, and peaks will form in the spectrum.

$$\begin{gathered}
\varphi = \frac{2\pi}{\lambda_k} n_1 d = k\pi (k = 1, 2, 3 \ldots) \\
k = \frac{2n_1 d}{\lambda_k} \\
(k+m) = \frac{2n_1 d}{\lambda_{k+m}} \\
m\lambda_k\lambda_{k+m} = 2n_1 d(\lambda_k - \lambda_{k+m}) \\
2n_1 d = \frac{m\lambda_k\lambda_{k+m}}{\lambda_k - \lambda_{k+m}}
\end{gathered} \tag{23}$$

(iii) In case of $n_0 < n_2 < n_1 \rightarrow R < 0$

When $\sin^2\varphi = 1$, the peaks will form.

$$\begin{gathered}
\varphi = \frac{2\pi}{\lambda_k} n_1 d = k\pi + \frac{\pi}{2} (k = 1, 2, 3 \ldots) \\
2k + 1 = \frac{4n_1 d}{\lambda_k} \\
2(k+m) + 1 = \frac{4n_1 d}{\lambda_{k+m}} \\
m\lambda_k\lambda_{k+m} = 2n_1 d(\lambda_k - \lambda_{k+m}) \\
2n_1 d = \frac{m\lambda_k\lambda_{k+m}}{\lambda_k - \lambda_{k+m}}
\end{gathered} \tag{24}$$

Eqs. (23) and (24) show that no matter $R > 0$ or $R < 0$, the films have the same thickness expression. Through the peak positions of Fabry–Pérot fringes, we can calculate the optical thickness of the film, the product of the physical thickness and refractive index.

Table 1
The relationship between the refractive index and the amplitude of the Fabry–Pérot fringes when the films are deposited on the quartz slides.

Refractive index of the film (n_1)	The amplitude of oscillation (A_B)
1.460	0
1.470	0.0023
1.480	0.0046
1.490	0.0069
1.500	0.0094
1.510	0.0119
1.520	0.0144
1.530	0.0170
1.540	0.0197
1.550	0.0224
1.560	0.0252

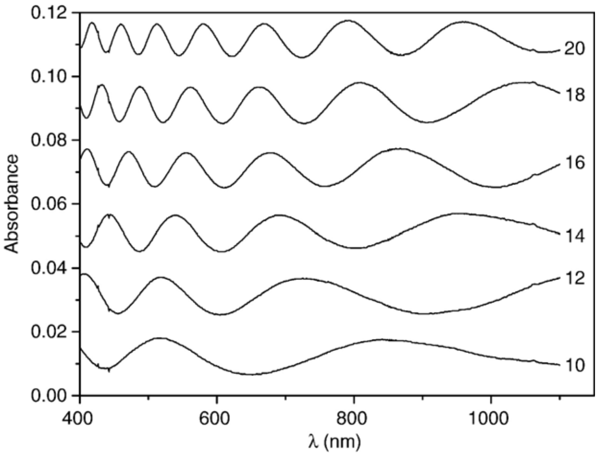

Fig. 4. Vis–NIR spectra of the (PVPON/PAA)$_n$ films for values of n varying from 10 to 20. (For clarity the spectra were transferred intentionally).

However, the amplitude of Fabry–Pérot fringes provides the information about refractive index. The amplitude is defined as below:

$$A = \mathrm{ABS}_{\max} - \mathrm{ABS}_{\min} \tag{25}$$

According to Eqs. (20), (21), and (22), the amplitudes of Situation A and B (Scheme 2) is given as below respectively

$$\begin{aligned}
A_A &= \left|\log\frac{(1+R)^2}{(1-R)^2}\right| = 2\left|\log\frac{1+R}{1-R}\right| \\
&= 2\left|\log\frac{n_1(n_0+n_2)}{n_0 n_2 + n_1^2}\right|
\end{aligned} \tag{26}$$

$$\begin{aligned}
A_B &= \left|\log\frac{(1+R)^4}{(1-R)^4}\right| = 4\left|\log\frac{1+R}{1-R}\right| \\
&= 4\left|\log\frac{n_1(n_0+n_2)}{n_0 n_2 + n_1^2}\right|
\end{aligned} \tag{27}$$

The PVPON/PAA film on one side of the quartz slide was removed by sodium hydroxide solution, which makes the system

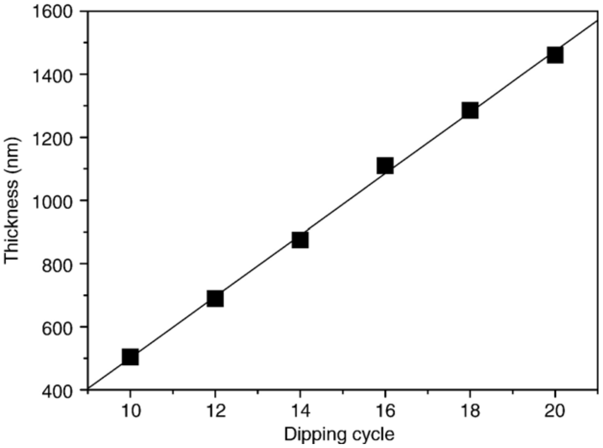

Fig. 5. Film thicknesses as a function of the assembling cycles. (The film is the same to that in Fig. 4. The film thickness was determined by Eq. (23) and Table 1).

changed from Situation B to Situation A. According to Eqs. (26) and (27), after the film on one side was removed, the amplitude would become the half of the original value. While according to Eqs. (23) and (24), after the removal, the peak position should not shift. These conclusions are proved by Fig. 3(a) and (b).

Eq. (26) or Eq. (27) indicates that the amplitude of the oscillations is determined by the refractive index of air, film and substrate. The refractive of air is considered as a constant value. When the same films are deposited on the different substrates, the difference in amplitude is determined by the refractive index of the substrate. The absorbance spectra of the PVPON/PAA films deposited on a glass and quartz slide are shown in Fig. 3 (b) and (c) respectively. The refractive index of the glass (~1.50) is very close to that of the PVPON/PAA film therefore the spectrum (c) has very weak amplitude. While due to the refractive index of the glass is larger than that of the quartz, the spectrum (b) has stronger amplitude than that of spectrum (c).

Generally, fluoride has very low refractive index. Here, LiF was deposited on a quartz slide under vacuum condition. For comparison, the LBL films on one side of the substrates (spectrum (b) and (c)) were removed. As shown in Fig. 3, the system (spectrum (d)) that LiF deposited on the quartz slide has the largest amplitude among them, owing to the striking difference between refractive indexes of the lithium fluoride (1.36 at 550 nm) and silicon dioxide (1.46 at 550 nm).

In Eq. (26) or Eq. (27), if let

$$y = \frac{n_1(n_0+n_2)}{n_0n_2+n_1^2}$$

then

$$\begin{aligned} \frac{dy}{dn_1} &= \frac{(n_0+n_2)(n_1^2-n_0n_2)}{(n_0n_2+n_1^2)^2} = 0 \\ n_1^2 - n_0n_2 &= 0 \\ n_1 &= \sqrt{n_0n_2} \end{aligned} \tag{28}$$

When $n_1 = \sqrt{n_0n_2}$, the amplitude will reach to maximal value. That is why the materials whose refractive index is equal to square root of the product of substrate and medium are selected to fabricate anti-reflectance film [21].

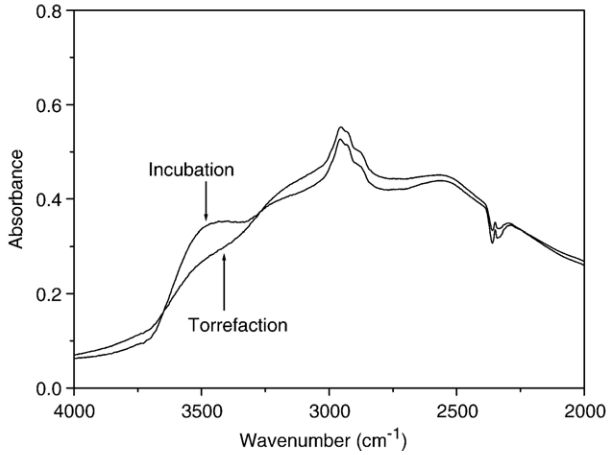

Fig. 6. FTIR spectra of a (PVPON/PAA)$_{16}$ film after one-day incubation in water (pH=2) at room temperature and after one-day torrefaction in a oven at 80 °C.

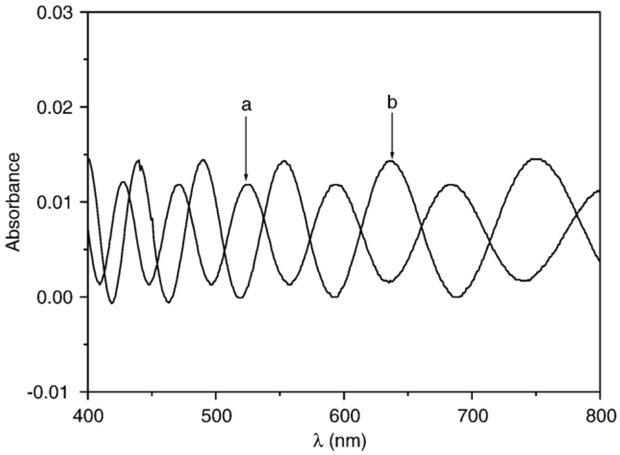

Fig. 7. Vis–NIR spectra of a (PVPON/PAA)$_{16}$ film: (a) after one-day incubation in water (pH=2) at room temperature; and (b) one-day torrefaction in a oven at 80 °C.

In Eq. (27), let

$$a = 10^{\frac{A_B}{4}}$$

When $R>0$

$$\begin{aligned} a &= \frac{n_1(n_0+n_2)}{n_0n_2+n_1^2} \\ an_1^2 - n_1(n_0+n_2) + an_0n_2 &= 0 \\ n_1 &= \frac{(n_0+n_2)\pm\sqrt{(n_0+n_2)^2-4a^2n_0n_2}}{2a} \end{aligned} \tag{29}$$

When $R<0$

$$\begin{aligned} a &= \frac{n_0n_2+n_1^2}{n_1(n_0+n_2)} \\ n_1^2 - an_1(n_0+n_2) + n_0n_2 &= 0 \\ n_1 &= \frac{a(n_0+n_2)\pm\sqrt{a^2(n_0+n_2)^2-4n_0n_2}}{2} \end{aligned} \tag{30}$$

Through Eqs. (29) and (30) two roots are got, but under the practical condition, one of them can be deleted. In our LBL system, the quartz slides are usually used as substrate. The refractive index of LBL film is usually larger than that of the quartz therefore $R<0$. The refractive indexes of air and quartz are 1.000 and 1.460 at wavelength of 550 nm respectively. For convenience, a table (Table 1) was presented according to Eq. (27). The amplitude can be read out through the spectrum of the LBL film, and then according to Table 1 the approximate value of the refractive index of the film can be estimated. (The dispersive effect is not taken into account here)

3.3. Monitoring of LBL film thickness

The UV–Vis–NIR spectra of the films made through different assembling cycles were record in Fig. 4. The more assembly cycles, the more oscillations present in the spectrum, indicating that the film becomes thicker as the assemble cycle increases.

The amplitude was read out to be 0.012, and therefore according to Table 1 and Eq. (30), the refractive index of the PVPON/PAA film was calculated to be about 1.510. Then according to Eq. (24), the thicknesses of the films with the different assembled cycles were determined. As shown in Fig. 5, from 10 to 20 assembling cycles, thickness of the films has a linear relationship with the assembly cycles. The film's average growth is 97 nm per assembly cycle, which is one the fastest increasing rates of LBL process have ever known [22].

3.4. Monitor the composition changes of film

Refractive index can be used as a parameter to determine the component content in the mixture system. Here, the LBL film can be looked as a polymer network filled with water. Therefore the film is divided into two parts, pure PVPON/PAA block and water. The effective index of the film can be estimated as [23]:

$$n_{1f} = v_p n_w + (1 - v_P) n_s \qquad (31)$$

where n_{1f} is the effective value of the refractive index of the water-filled film, n_w is the refractive index of water , and n_s is the refractive index of the of the pure PVPON/PAA block. v_p is the water volume fraction of the water-absorbed film.

The newly fabricated $(\text{PVPON/PAA})_{16}$ film was incubated in water (pH = 2) for a day. Then the film was torrefied in an oven at 80 °C for a day. The FTIR spectra proved that the incubation and torrefaction can prepare high and low water content samples respectively. As shown in Fig. 6, torrefaction led the strength of shoulder peak at $\sim 3500\ \text{cm}^{-1}$ assigned to O–H stretching vibration of water to become weak, indicating there were water molecules driven out by torrefaction.

According to Eq. (31), because $n_w < n_s$, when the water content in the film reduces, the effective index of the film will increase. According to Table 1 or Eq. (27), the increase of refractive index film would amplify the amplitude of Fabry–Pérot fringes. This conclusion is proved by Fig. 7. The sample with high water content (Fig. 7, Spectrum a) has weaker amplitude than that of the sample with low water content (Fig. 7, Spectrum b). When the water content of the film changes, the effective index of the film will change, and correspondingly the amplitude of Fabry–Pérot fringes will change. Therefore the amplitude can be used as an indicator of the composition change of the LBL film.

4. Conclusion

If the obvious refractive index contrast between the film and substrate exists, when the LBL films reach to certain thickness and have high level of smoothness, the Fabry–Pérot fringes will display in the UV–visible spectra of the films. The peak positions of Fabry–Pérot fringes are determined by the product of the refractive index and thickness of the film, while the amplitude is determined by the refractive index contrast between film and substrate.

Through the peak positions and the amplitude of the Fabry–Pérot fringes, the thickness and refractive index of the film can be evaluated. At the same time, the amplitude can be used as an indicator of the composition change of the film.

Acknowledgments

This work was financially supported by the National Natural Science Foundation of China (Grant No. 50425312 and No. 50521302). Authors thank Dr. Xinjun Xu (Lab of Organic Solid, Institute of Chemistry) for help with preparation of LiF film.

References

[1] G. Decher, J.D. Hong, J. Schmitt, Thin Solid Films 210 (1992) 831.
[2] G. Decher, Science 277 (1997) 1232.
[3] P. Bertrand, A. Jonas, A. Laschewsky, R. Legras, Macromol. Rapid Commun. 21 (2000) 319.
[4] P.T. Hammond, Curr. Opin. Colloid Interface Sci. 4 (1999) 430.
[5] M. Schonhoff, Curr. Opin. Colloid Interface Sci. 8 (2003) 86.
[6] W.B. Stockton, M.F. Rubner, Macromolecules 30 (1997) 2717.
[7] L. Wang, Z. Wang, X. Zhang, J. Shen, L. Chi, H. Fuchs, Macromol. Rapid Commun. 18 (1997) 509.
[8] Y. Shimazaki, M. Mitsuishi, S. Ito, M. Yamamoto, Langmuir 13 (1997) 1385.
[9] Y. Zhang, W. Cao, Langmuir 17 (2001) 5021.
[10] E. Hao, L. Wang, J. Zhang, B. Yang, X. Zhang, J. Shen, Chem. Lett. (1999) 5.
[11] H. Xiong, M. Cheng, Z. Zhou, X. Zhang, J. Shen, Adv. Mater. 10 (1998) 529.
[12] J. Sun, T. Wu, Y. Sun, Z. Wang, X. Zhang, J. Shen, W. Cao, Chem. Commun. (1998) 1853.
[13] J. Chen, G. Luo, W. Cao, Macromol. Rapid Commun. 22 (2001) 311.
[14] S.A. Sukhishvili, S. Granick, Macromolecules 35 (2002) 301.
[15] Y. Lvov, G. Decher, Crystallogr. Rep. 39 (1994) 628.
[16] R.A. McAloney, M. Sinyor, V. Dudnik, M.C. Goh, Langmuir 17 (2001) 6655.
[17] S. Yan, Z. Chen, Z. Song, Q. Pao, Water Soluble Polymer (in Chinese), Chemical Industry Press, Beijing, 1988 Chapter 4.
[18] S. Yang, Y. Zhang, L. Wang, S. Hong, Y. Chen, J. Xu, C. Li, Langmuir 22 (2006) 338.
[19] C. Lau, Y. Mi, Polymer 43 (2002) 823.
[20] Y. Lin, W. Lu, Optics of Thin Film (in Chinese), Defense Industry Press, Beijing, 1990 Chapter 1.
[21] J. Hiller, J.D. Mendelsohn, M.F. Rubner, Nat. Mater. 1 (2002) 59.
[22] S.T. Dulas, J.B. Schlenoff, Macromolecules 32 (1999) 8153.
[23] L. Zhai, A.J. Nolte, R.E. Cohen, M.F. Rubner, Macromolecules 37 (2004) 6113.